IEEE Access
Multidisciplinary | Rapid Review | Open Access Journal

Date of publication xxxx 00, 0000, date of current version xxxx 00, 0000.

Digital Object Identifier 10.1109/ACCESS.2017.Doi Number

Antenna for Ultra-Wideband Applications with Non-Uniform Defected Ground Plane and Offset Aperture-Coupled Cylindrical Dielectric Resonators

C. Zebiri[1,2], D. Sayad[3], I.T.E. Elfergani[4], J. Kosha[2], W.F.A. Mshwat[2], C. H. See[5], M. Lashab[6], J. Rodriguez[4], K. H. Sayidmarie[7], H.A. Obeidat[2] and R.A. Abd-Alhameed[2,8]

[1]Department of Electronics, University of Ferhat Abbas, Sétif -1-, 19000 Sétif, Algeria
[2]School of Electrical Engineering and Computer Science, University of Bradford, BD71DP, UK
[3]Department of Electrical Engineering, University of 20 Aout 1955-Skikda, 21000 Skikda, Algeria.
[4]Instituto de Telecomunicações, Campus Universitário de Santiago, Aveiro, Portugal
[5]School of Engineering and the Built Environment, Edinburgh Napier University, UK.
[6]Department of Electronics, University of Oum-elbouagui, 4000 Oum-elbouagui, Algeria
[7]College of Electronic Engineering, Ninevah University, Mosul 41002, Iraq
[8]Information and Communication Engineering Department, Basrah University College of Science and Technology, Basrah 24001, Iraq

Corresponding author: Raed A Abd-Alhameed (e-mail: r.a.a.abd@bradford.ac.uk).

This work was supported in part by the Innovation Programme under Grant H2020-MSCA-ITN-2016 SECRET-722424 and in part by the U.K. Engineering and Physical Sciences Research Council (EPSRC) under Grant EP/E022936/1.

ABSTRACT A new compact Cylindrical Dielectric Resonator Antenna (CDRA) with a defected ground for ultra-wideband applications is presented. The structure is based on two cylindrical dielectric resonators asymmetrically located with respect to the center of an offset rectangular coupling aperture, with consideration of three and four Dielectric Resonators (DR). The resonant modes generated by the defected ground are studied and investigated. A parametric optimization study of the antenna design has been carried out to determine the optimal dimensions of the defected ground plane, resulting in an impedance bandwidth of over 133% that covers the frequency band from 3.6 GHz to 18.0 GHz. A power gain of about 7.9 dBi has been achieved. Design details and measured and simulated results are presented and discussed.

INDEX TERMS Cylindrical Dielectric Resonators Antenna, Ultra-Wideband, Defected Ground Structure

I. INTRODUCTION

Recently, the Defected Ground Structure (DGS) technique has received much attention in the design of microwave and millimeter wave sub-systems. It consists of etching variously shaped apertures in the ground plane to create a disturbance in the current distribution [1], [2]. For more than a decade, frequency-selective properties of DGSs have been widely used in printed circuits and antenna applications. DGS were first proposed for antenna applications in 2005 [3]. Among other benefits, the technique can reduce cross-polarization, which constitutes a major drawback for some wideband antennas [4].

In recent studies, the DGS technique is mainly employed to improve the impedance bandwidth of patch antenna structures [1]. Similar topics were treated in [2], [4], [5]. This technique can also be used to reduce coupling [6], minimize the structure size, and excite additional resonance modes using simple and compact DGSs configurations [7], [8]. It can be used to achieve single-feed multi-frequency microstrip antennas, including multiband functions using various DGSs [9], [10]. Moreover, the use of DGS can also enhance the antenna gain [2], [11], [12]. In this context, DGSs of many shapes have been investigated, such as circles, spirals, concentric rings, elliptical dumbbells and U and V slots [2]-[4]. Shapes such as rectangular, square, or semi-circular arcs [1] with varying dimensions can provide particular improvements in DGS-based antenna performances [4]. DGS has been used in controlling active microstrip antennas [4]. In [13] and [14], DGSs were used to design desired dual and triple band-notched UWB antennas.

This article has been accepted for publication in a future issue of this journal, but has not been fully edited. Content may change prior to final publication. Citation information: DOI 10.1109/ACCESS.2019.2949527, IEEE Access

In [15], a shovel-shaped DGS was used in a simple and compact UWB planar monopole antenna with filtering characteristics. In [16], a simple CPW-fed monopole patch antenna surrounded with a coplanar ground plane was presented. Further modifications of the DGS was made to enhance the gain and impedance bandwidth [16]. This technique was extended to Dielectric Resonator Antennas (DRAs), where the mutual coupling between two circular microstrip patches was suppressed making use of the stop-band property of the proposed DGS.

DRAs have emerged as a novel radiation technology, with the advantage of having high efficiency. Consequently, special DRA shapes and multi-segment DRAs have been reviewed extensively. Rectangular [17], Conical [18], asymmetrical E [19], Stair-Shaped [20], Inverted L-shaped [21], elliptical [22], asymmetrical T-shaped [23], tetrahedral [24] with triangular slot [25], ring-shaped [4] cylindrical [2] [26]-[28], and hybrid hemispherical-conical-shaped [29] configurations have all been suggested for antenna bandwidth enhancement. Gain and bandwidth enhancement configurations were presented in [2] and [30], where two cylindrical dielectric resonators were asymmetrically placed around the center of the rectangular coupling aperture, and fed through this defected ground plane aperture. In [30], a parametric optimization study was carried out and a bandwidth of about 57% was achieved, covering 8.02 to 14.55 GHz with a 10 dBi power gain. These results are quite comparable to those found in [2], namely a bandwidth of about 54%, a frequency band from 8.5 to 14.7 GHz and a 12 dBi gain.

Currently, the operating bandwidth of antennas using DRAs has been further improved for ultra-wideband applications [29], [30], [31]. In [32], a mono-cylindrical Dielectric Resonator (DR) was fed using two crossed slots centered at different locations. The slot modes were considered partially independent from the DR mode; in consequence, a wide bandwidth is attained. In [2], [26] and [30], wideband slot-fed asymmetric DRAs analyses were presented, where two adjacent cylindrical dielectric resonators were placed asymmetrically around the rectangular feeding aperture. The asymmetrical locations provide a further optimization parameter in the DRA design. As a result, the proposed antenna parameters are significantly improved: a 29% impedance bandwidth, a 9.62 to 12.9 GHz frequency band and an 8 dBi realized gain were achieved [26].

The present paper extends our recent work [27], which presented a compact ultra-wideband DRA using two cylindrical dielectric resonators asymmetrically placed near the center of an offset rectangular coupling aperture; this resulted in a 62% bandwidth, covering the two bands 5.9 to 7.32 GHz and 8.72 to 16.57 GHz, with a gain of 8 dBi. Herein, using the same aperture concept, the relative bandwidth is increased up to 133.33% covering the frequency range from 3.6 to 18 GHz. This range covers C band (4 to 8 GHz), X band (8 to 12.4 GHz) and Ku band (12.4 to 18 GHz), comprising services such as earth-to-satellite bands at 5.9 to 6.4 GHz, 12.25 to 13.25 GHz and 14 to 14.5 GHz, connections for satellite-earth at 10.7 to 11.7 GHz, 10.5 GHz for police radar and, for commercial use, 10.7 to 13.2 GHz.

The current basic design is a defected ground plane microstrip-fed DRA obtained by modifying the initial design in [27] achieving further enhancements in impedance bandwidth and gain. Experimental and simulation results of the resulting novel antenna are presented and discussed. The present work mainly intended to improve our recently published work [27], where the bandwidth is improved twice by use of DGS technique. The novelty of this work, hence, lies in the combination of the DGS with the DRA structures.

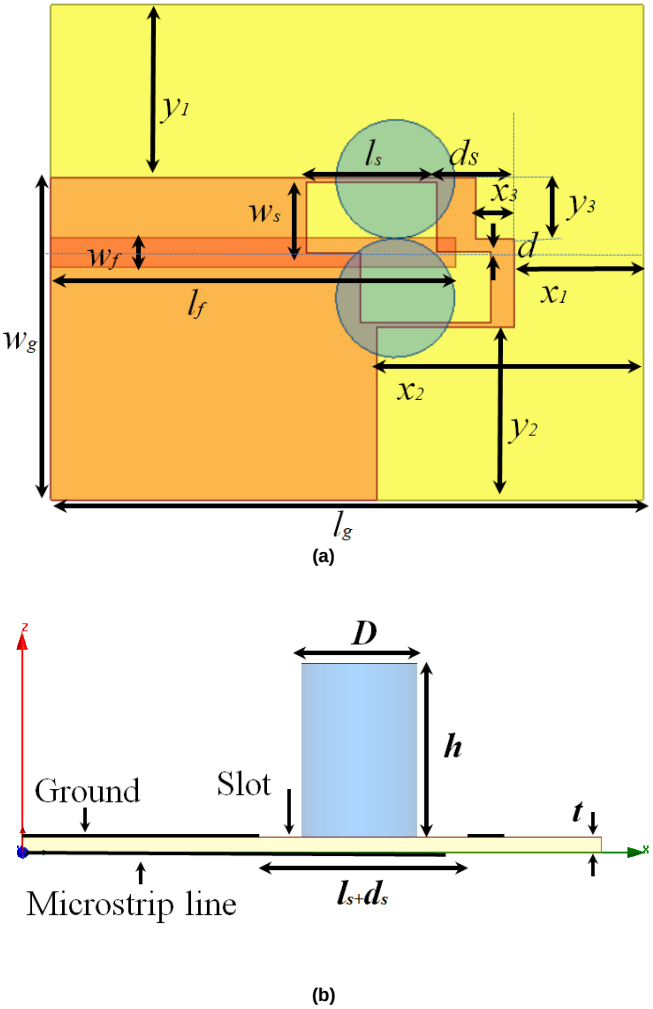

FIGURE 1. Design parameters of two aperture-coupled DRAs with non-uniform defected ground plane, (a) top view and (b) side view.

II. PROPOSED ANTENNA GEOMETRY AND SUMMARIZED RESULTS

The geometry of the basic monopole antenna design is shown in Fig. 1. A microstrip feed is used due to its impedance matching simplicity and other useful features

[27]. The proposed asymmetric ultra-wideband antenna with a defected ground plane is designed and realized on an FR4 30×25×0.8 mm^3 substrate with relative permittivity ε_{rs}=4.4 and 0.017 loss tangent. Two identical alumina-96%-DRs of radius D =6 mm and height h =9 mm have been used. A feeding microstrip line of length l_f =20.5 mm and width w_f=1.5 mm is located symmetrically around the coupling aperture. Its dimensions were calculated using empirical formulas [2], [26], [27], [30], [32].

Simulations for this geometry were carried out using HFSS software. Two identical rectangular apertures (slots) of length l_s and width w_s are etched on the ground plane, shifted from the center by a distance d. Based on the experimental results obtained in [27], a stub length close to $\lambda_g/4$ is also used in this design, although this differs from that of [27] by including the ground plane apertures. The final antenna dimensions (Fig. 1) are w_f=1.5 mm, l_f=20.5 mm, w_s=3.5 mm, l_s=6.6 mm, d_s =3.1 mm and d=0.2 mm are optimized in our previous work [27], and the dimensions of the defected antenna are w_g=16.25 mm, l_g=16.5 mm, x_1=6.5 mm, x_2=13.5 mm, x_3=1.5 mm, y_1=8.75 mm, y_2=8.75 mm and y_3 =3.15 mm.

III. CHARACTERISTIC MODES DESCRIPTIONS

Building on previous works [2], [26], [30], [27], modifications are applied to the basic antenna according to the realization steps of our model shown in Fig. 2(a). The originality of this work lies in the creation of a defected ground plane for exciting further modes [2] and enhancing the bandwidth and gain. The segmentation of the ground plane improves the return loss S_{11} as illustrated in Fig.2(b).

As shown in Table I, all four proposed designs (ii) to (v), presented in Fig. 2(a), have a bandwidth greater than that of antenna (i) presented in [27]. The application of the DGS technique has led to a single band extending from 3.6 to 18 GHz, *i.e.* a 133.33 % relative bandwidth. It should be noted that the major improvement achieved by this technique occurs below 10 GHz (3.6-10 GHz). The introduction of the defected ground to the slotted structure (Antenna (i) [27]) led to the appearance of other resonance frequencies between 3.6 and 6 GHz, and from 6 to 10 GHz due to the combined effect of the DRA and the slotted defected ground.

TABLE I
BANDWIDTH OF THE FIVE DESIGNS SHOWN IN FIG. (2.A).

Design	BW (GHz)	BW (%)
i[27]	5.9-7.4 and 9.1-17.8	22.56 and 64.68
ii	5.5-7.3 and 9-17.8	28.13 and 65.67
iii	5.6-7.6 and 8.3-17.8	30.30 and 72.79
iv	3.7-17.9	131.48
Prototype	3.6-18	133.33

Although the existing literature clearly favors probe excitation at lower frequencies where coupling apertures are not often used due to their large size [33], [34], in our case, large slots, when combined with the DGS technique, has shown better excitation performances for a two DR structure. This combination is considered as the main novelty of this work.

Generally, isolated cylindrical DRAs support TE, TM and hybrid resonant modes [28], [35], [36], in a widely adopted designation. Amongst multiple cylindrical DRA modes, the $TE_{01\delta}$, $TM_{01\delta}$, and hybrid $HEM_{11\delta}$ (with dominant E_z component) modes are the most commonly considered radiating modes. The subscript numbers in the mode designation express the field variation in the azimuth, radial and axial directions, respectively. The index δ, lying between 0 and 1, indicates the resonant behavior along the dielectric cylinder height (z axis). The $TE_{01\delta}$ mode, $TM_{01\delta}$ mode and $HEM_{11\delta}$ mode radiate similarly to the short vertical magnetic dipole, short vertical electric dipole and short horizontal magnetic dipole, respectively [36].

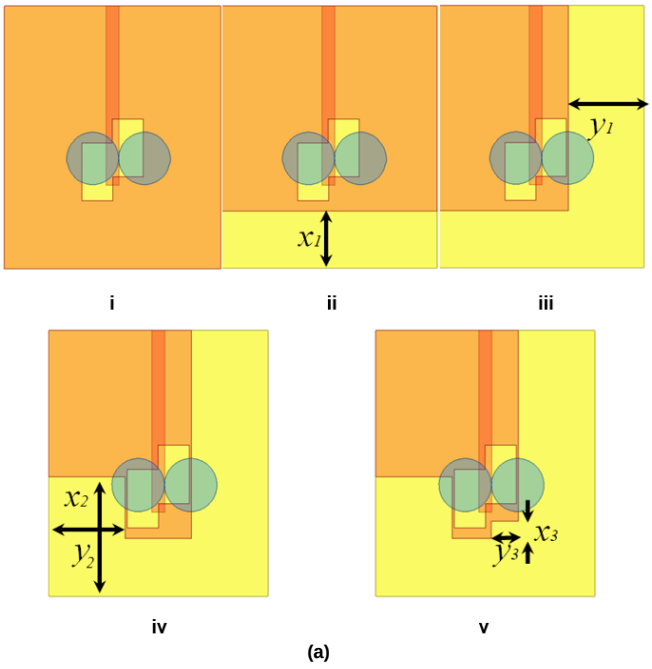

(a)

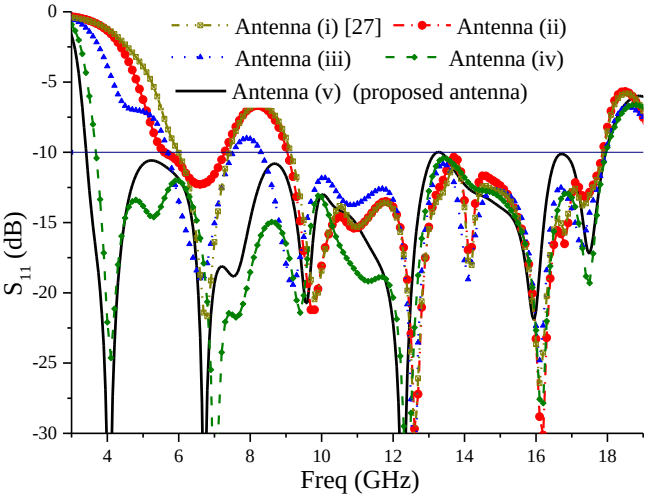

(b)

This article has been accepted for publication in a future issue of this journal, but has not been fully edited. Content may change prior to final publication. Citation information: DOI 10.1109/ACCESS.2019.2949527, IEEE Access

FIGURE 2. (a) Evolution of the proposed antenna, (i) the design of [27], (ii), (iii),(iv), (v) steps of design optimization. (b) simulated S_{11} of the five designs shown in (a).

In our case, a large double slot is etched in the ground plane, resulting in multiple magnetic/electric modes over frequency. The slot has more effect depending on the frequency; it resonates at low frequencies exciting the DRA at 10 and 12, and up to 16 GHz, (Fig. 2).

Much research has focused on cylindrical DRAs [28], [37]-[40]. In [38] and [39], the DRA device is used as sensors for wireless networks and liquid chemical detection applications, respectively. In these structures, the TM and quasi-TM modes can be excited by placing the dielectric disk on the ground plane [41]. Little attention has been paid to the TE and quasi-TE modes, which cannot be excited when the base of the DRA is placed on the ground plane [42]. In [42], some DRA $HEM_{11\delta}$ and $HEM_{12\delta}$ mode features, compared to the most widely studied $TM_{01\delta}$ and $TE_{01\delta}$ modes, are briefly discussed. The resonant frequency f_o of the $TE_{01\delta}$ mode, $TM_{01\delta}$ mode, and $HEM_{11\delta}$ are respectively given by the following empirical equations [36], [43], [44]:

$$f_{0/TE_{01\delta}} = \frac{2.327c}{2\pi \cdot a \cdot \sqrt{\varepsilon_r + 1}} \left(1 + 0.2123\frac{a}{h} - 0.00898\left(\frac{a}{h}\right)^2\right) \quad (1)$$

$$f_{0/TM_{01\delta}} = \frac{c}{2\pi \cdot a \cdot \sqrt{\varepsilon_r + 2}} \sqrt{3.83^2 + \left(\frac{\pi \cdot a}{2 \cdot h}\right)^2} \quad (2)$$

$$f_{0/HEM_{11\delta}} = \frac{6.324c}{2\pi\sqrt{\varepsilon_r + 2}} \left(0.27 + 0.36\frac{a}{2h} + 0.02\left(\frac{a}{2h}\right)^2\right) \quad (3)$$

where ε_r is the DR relative permittivity, a is the radius and h is the height of the dielectric cylinder. Note that there are neither exact mathematical expressions for the resonant frequencies of higher order modes nor exact solutions for their internal fields and radiation patterns [36]. An approximate solution for the cylindrical DRAs field pattern has been obtained by considering a magnetic wall boundary condition on the surfaces parallel to the z axis [45].

The slot length is calculated using the following [44]:

$$L = \frac{c}{2f_0}\sqrt{\frac{2}{\varepsilon_r + \varepsilon_{rs}}} \quad (4)$$

where ε_r and ε_{rs} are the relative dielectric constant of the DR and substrate, respectively. In [46], measurements of the cylindrical dielectric resonator $HEM_{11\delta}$ mode radiation efficiency for $\varepsilon_r = 38$ show values better than 98%.

The slot in our case (with wide zigzag) has changed the shape of the magnetic current (magnetic dipole), and excited other modes at low frequencies (less than 10 GHz) (Fig. 2(b)). Equations (1-7) of the resonant frequency modes were derived from the calculations of the cylindrical dielectric resonator by considering perfect electric and/or magnetic walls on the resonator faces. The perfect magnetic wall condition was shown to be accurate for higher ε_r values [47], but remains fairly valid for lower values.

The three first modes $TE_{01\delta}$, $TM_{01\delta}$, and $HEM_{11\delta}$ resonant frequencies of the cylindrical resonator are given by the following empirical expressions [33]:

$$f_{0/TE_{01\delta}} = \frac{c \cdot 2.921}{2\pi \cdot a \cdot \varepsilon_r^{0.456}} \left(0.691 + 0.319\frac{a}{2h} - 0.035\left(\frac{a}{2h}\right)^2\right) \quad (5)$$

$$f_{0/TM_{01\delta}} = \frac{c \cdot 2.933}{2\pi \cdot a \cdot \varepsilon_r^{0.468}} \left(1 - \left(0.075 - 0.05\frac{a}{2h}\right)\left(\frac{\varepsilon_r - 10}{28}\right)\right) \times \left(1.048 + 0.377\left(\frac{a}{2h}\right) - 0.071\left(\frac{a}{2h}\right)^2\right) \quad (6)$$

$$f_{0/HEM_{11\delta}} = \frac{c \cdot 2.735}{2\pi \cdot a \cdot \varepsilon_r^{0.436}} \left(0.543 + 0.589\frac{a}{2h} - 0.050\left(\frac{a}{2h}\right)^2\right) \quad (7)$$

where a and h arethe DR radius and height, respectively.

The differences between these equations are clarified by an example in Table II, as these equations do not include any information about the coupling factor or the quality factor of CDRA and the approximation is given with respect to ratio (a/h).

The DRA resonant frequency can be controlled by varying the length of the slot, which may also help in reconfiguring the radiation patterns.

When a single shaped DRA operates in the fundamental mode, its bandwidth typically does not exceed 10% [48]. Experimental work on wide-band DRAs was described in 1989 by Kishk *et al.* [48] who proposed using two separate DRAs stacked end to end to achieve a dual-resonance band. Other wideband configurations using this technique have since been reported [49]-[51].

An alumina-96% based DRA (ε_r = 9.4) has been designed with a diameter D = 6 mm and a height h = 9mm. The resonant frequency of a single segment CDRA excited in $HEM_{11\delta}$ mode is given by [26], [27]

$$f_0(GHz) = \frac{c}{2\pi \cdot a \cdot \sqrt{\varepsilon_r}} \left(1.71 + \frac{a}{h} + 0.1578\left(\frac{a}{2h}\right)^2\right) \quad (8)$$

where $a = D/2$ (in cm), c is the free space light velocity. For these dimensions, the calculated frequency is 10.63 GHz. The DRs are asymmetrically placed around the asymmetrical slots, hence, the DRA modes depend on the DR geometrical parameters, the permittivity and the feeding mechanism. The asymmetric DR pair configuration and the dimensions and shape of the defected ground give designers more scope for functional optimization. In this study, a 133% impedance bandwidth, covering 3.6 GHz to 18.0 GHz, has been achieved.

TABLE II
BANDWIDTH OF THE FIVE DESIGNS SHOWN IN FIG. (2.A).

Design	BW (GHz)	BW (%)
Equ (1)/TE	1.2285e+10	0.3177
Equ (5)/TE	1.2437e+10	
Equ (2)/ TM	1.8222e+10	1.2171
Equ (6)/TM	1.8193e+10	
Equ (3)/ HEM	9.9366e+09	6.0101
Equ (7)/ HEM	1.0484e+10	
Equ (7)/ HEM	1.0484e+10	1.3728

This article has been accepted for publication in a future issue of this journal, but has not been fully edited. Content may change prior to final publication. Citation information: DOI 10.1109/ACCESS.2019.2949527, IEEE Access

Equ (8)/HEM 1.0630e+10

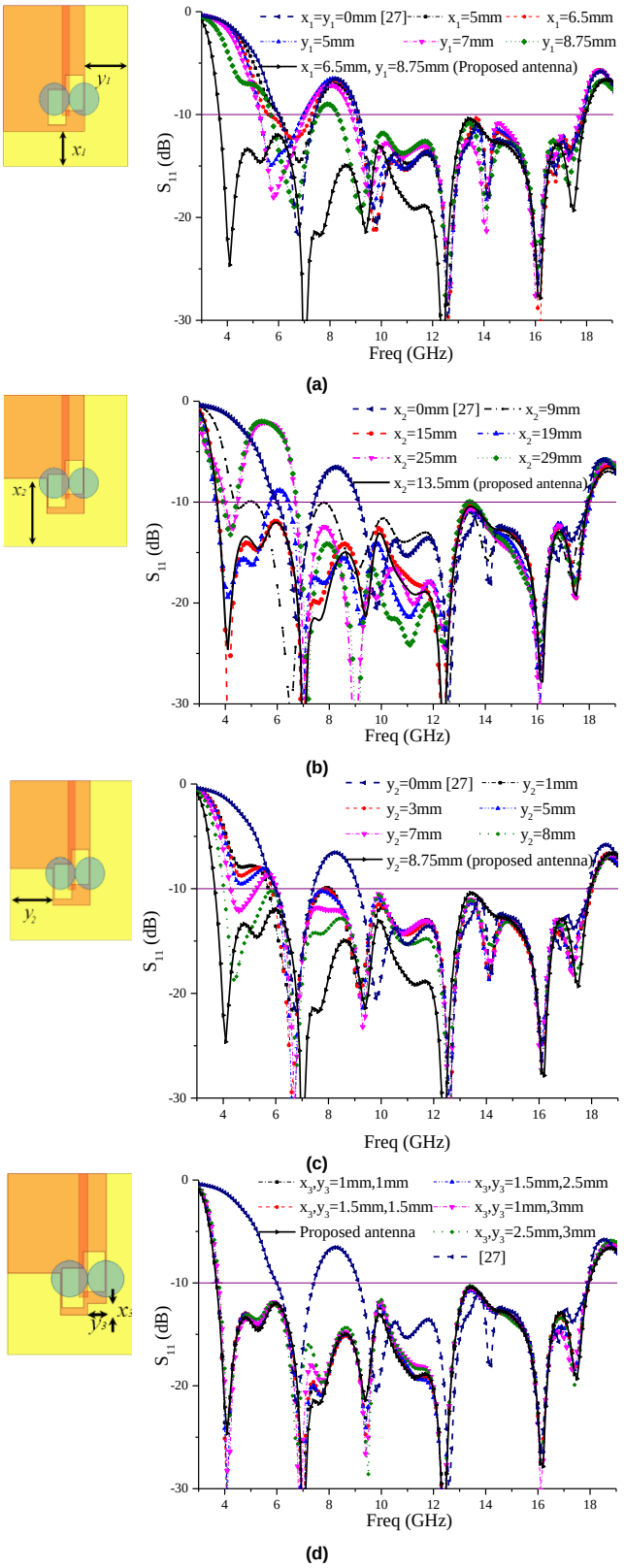

FIGURE 3. Effect of different slit lengths on S_{11} of the aperture-coupled asymmetric DRA with DGS, compared with the proposed antenna and with the antenna in [27]. (a) Effect of slit length x_1 (y_1=0mm) and the effect of the slit length y_1 (x_1=6.5mm), (b) Effect of the slit length x_2 (x_1=6.5mm and y_1=y_2=8.75mm), (c) Effect of the slit length y_2 with x_1=6.5mm, y_1=8.75mm and x_2=13.5mm, (d) Effect of the slit x_3×$y_3$with x_1=6.5mm, y_1=8.75mm and x_2=13.5mm.

Table II compares the results of the 7 equations mentioned above for a = 3 mm, h = 9 mm and ε_r = 9.4. The resonant frequencies of dielectric resonators are determined using rigorous numerical methods [43].

According to ε_r and a/h, closed-form expressions for different modes are obtained. The accuracy of the formulas presented above (Equations 1-8) is demonstrated for the same resonator parameters for which the results of rigorous numerical methods available in the literature are very close [43]. Let us conclude this part with a comparison of the size of our antenna with those realized or simulated available in the literature.

TABLE III
ANTENNA DIMENSIONS AND PROPERTIES COMPARISON WITH PUBLISHED DATA.

Reference, Year	Total Area (mm^3)	Operating bands(GHz)	Gain dBi
[23], 2012	60×60×13.6	3.81 to 8.39	3-24-7.75
[29], 2012	70×70×11	4-16	2–4
[18], 2013	100×100×20	3.5-10.5	4.25-8.3
[26], 2014	30×25×9.8	9.62-12.9	6-8
[19], 2016	50×50×5.8	6.0–10.2	4.5-8.1
[20], 2016	27×25×6.8	3.844-8.146	3-3.9
[30], 2016	30×25×9.8	9.1-14.6	6.2-8
[2], 2017	30×25×9.8	8.02-14.55	6-12
[21], 2017	44×44×10.8	3.76-9.35	5-8
[25], 2017	140×140×5.8	3.8–8.1	5.5 to 7.5
[27], 2017	30×25×9.8	5.9-7.32/8.7-15	6-12
[22], 2018	80×80×9	8.26 - 12.15	6.2-8.1
[28], 2019	120×120×12	2.33-2.52	6.2
Our proposed antenna	30×25×9.8	3.6-18	6-8

It is clear from Table III that our proposed structure presents a good compromise between miniaturization and the significant gain obtained compared to the reported studies.

Fig. 3(a) shows the ground plane length effect on the reflection coefficient. It is clearly seen that it acts most strongly on frequencies below 10 GHz. In this case, the optimal value for x_1 is 6.5 mm. The width of the second truncation (y_1) is in the y-direction. It is noted that the effect is clearly visible in the frequency band 3-10 GHz. In this case, the impedance matching is better at y_1 = 8.75 mm, where the mismatch between 7 and 10 GHz decreases with respect to y_1 and is optimal for y_1 = 8.75 mm for frequencies beyond 10 GHz, which are less affected by the truncation of the ground plane.

Fig. 3(b) shows that increasing x_2 up to 13.5 mm improves the bandwidth. Beyond 17 mm, a mismatch is observed for lower frequencies. From Fig. 3(c), we note that for x_2 = 13.5 mm with varying y_2, a further bandwidth improvement is obtained for y_2=8.75 mm. In Fig. 3(d), the effect of the truncation x_3×y_3 is not clearly visible, but in reality, a slight increase of 1% in bandwidth for x_3×y_3 =1.5mm×3.15mm is obtained.

To validate the simulated results, an antenna prototype is constructed as shown in Fig. 4(a), and its parameters

This article has been accepted for publication in a future issue of this journal, but has not been fully edited. Content may change prior to final publication. Citation information: DOI 10.1109/ACCESS.2019.2949527, IEEE Access

were measured using a vector network analyzer. The measurement of the proposed antenna with and without DRs results are also compared and are in good agreement with the simulation ones.

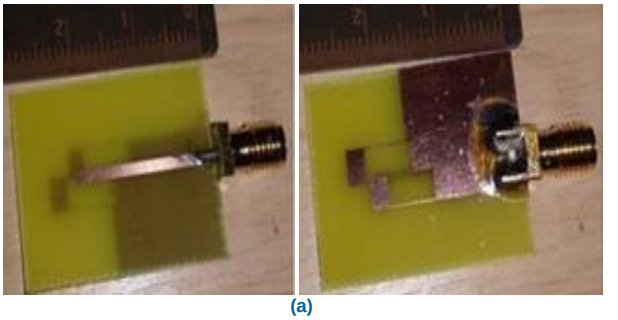

(a)

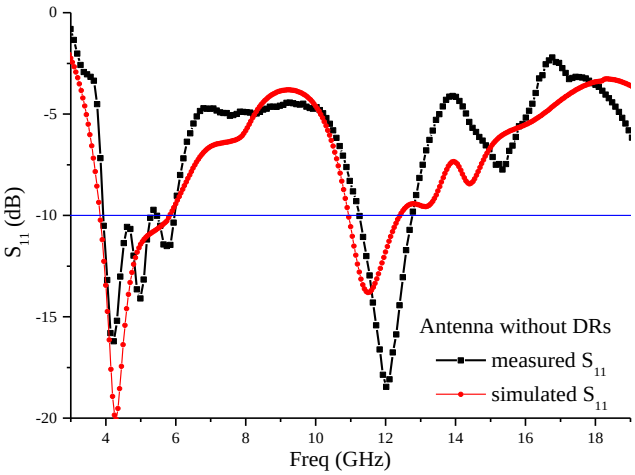

(b)

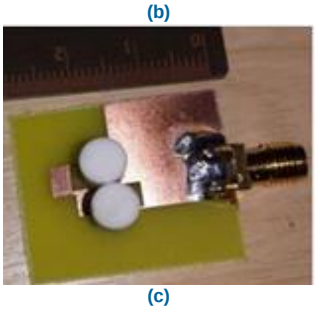

(c)

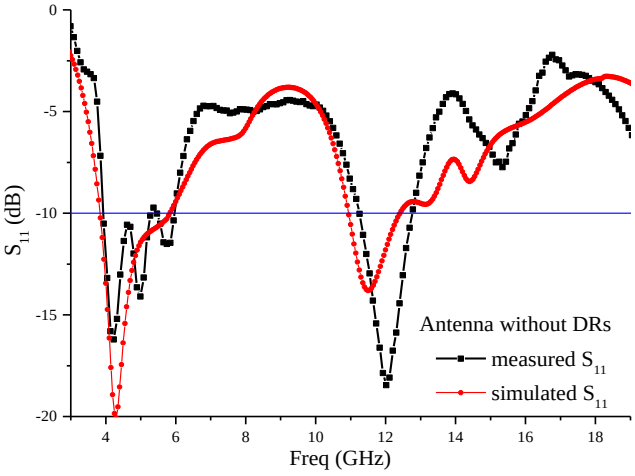

(b)

FIGURE 4. Proposed antenna. (a) antenna faces photograph without DR, (b) Measured and simulated reflection coefficient of the antenna without DR (c) our proposed antenna photograph with two DRs, (d) Measured and simulated reflection coefficient of the proposed antenna with DR (with glue of various thicknesses t)

Fig. 4(b) shows good agreement between measurements and simulations of the antenna without DR. We can notice that this antenna works in the frequency bands 3.9-6GHz and 11.1-12.8GHZ only by the application of the DGS and the slot techniques without the introduction of the DR. Figs. 4 (c) and (d) present the prototype of the antenna with DR and the simulated and measured S_{11} without and with consideration of the glue thickness, respectively. It is remarkable with confirmation that the glue has a considerable effect on S_{11}, especially at high frequencies. In general, the obtained results are in good agreement.

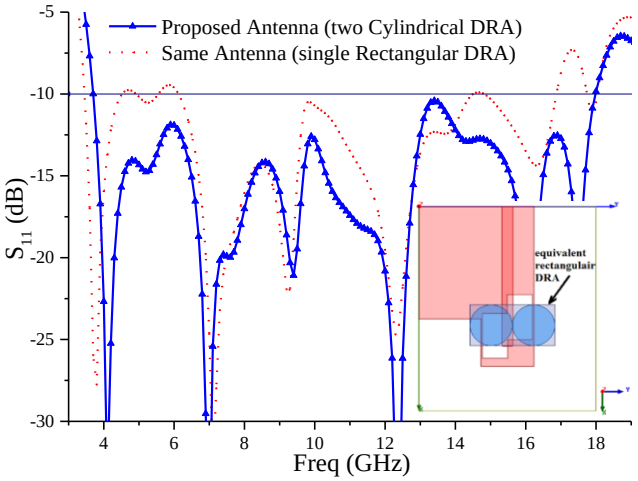

(a)

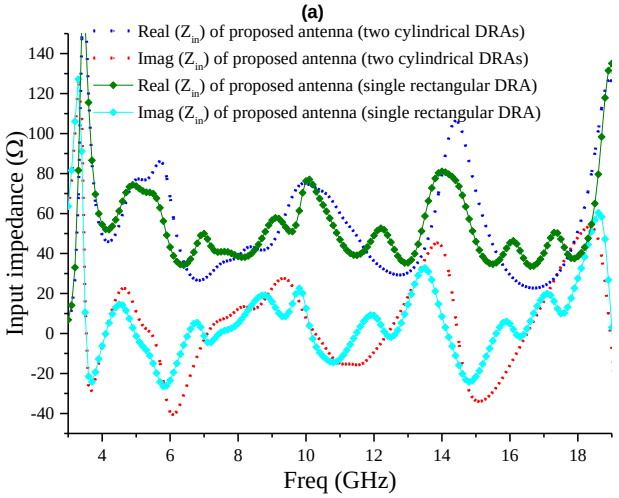

(b)

FIGURE 4. (a) Simulated S_{11} of 2-cylindrical DRA compared to a single rectangular DRA with the same overall dimensions, (b) Simulated input impedance of 2-cylindrical DRA compared to a single rectangular DRA.

Figs. 5(a) and (b) show the benefit of the introduction of the cylindrical DR to excite more hybrid modes than with a rectangular DR, as was previously reported in [27].

According to [33], the frequencies of the three lowest modes $HEM_{01\delta}$, $TE_{01\delta}$ and $TM_{01\delta}$ of a single cylindrical

This article has been accepted for publication in a future issue of this journal, but has not been fully edited. Content may change prior to final publication. Citation information: DOI 10.1109/ACCESS.2019.2949527, IEEE Access

DRA are 10.484, 12.188 and 18.164 GHz, respectively, while in [43], [53] the resonant frequencies for $HE_{11\delta}$, $EH_{11\delta}$, $TE_{11\delta}$ and $TM_{01\delta}$ modes are 9.8469, 10.2358, 12.2768 and 18.2089 GHz, respectively. These modes are only excited by a single DRA, so it is possible for other modes to be excited at low frequencies by the two DRAs (the same effect as for the rectangular DRA in [27]).

It should be noted that in this study, the ground plane used is defected while a full sized plane is used in [27].

The presented results give an additional proof to the equivalence between the two cylindrical DR's with a single rectangular DR having the same overall dimensions.

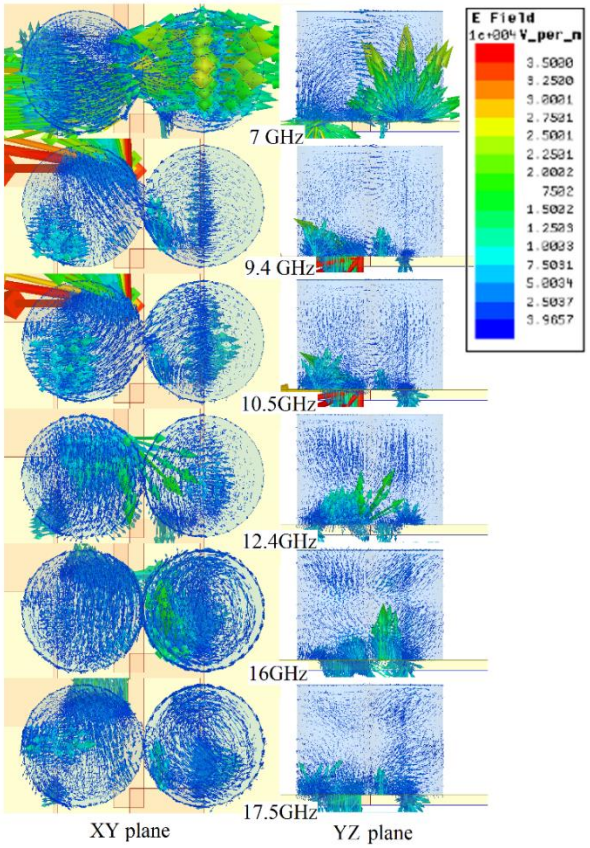

FIGURE 6. Magnitude of electric field distribution for 7.0 GHz and (TEδ11, quasi-HE11δ) 9.4 GHz, 10.5GHz (HEM01δ, EH11δ, TE1δ1, and TE11δ) 12.4 GHz (TE01δ), 16.0 GHz (TE102 and TEδ21) and 17.5 GHz (TM01δ).(xz plane, yz plane).

For the case of a single rectangular DR, according to [54] and [27], the frequencies of $TE_{\delta 11}$, $TE_{1\delta 1}$ and $TE_{11\delta}$ modes are 7.19, 10.23 and 10.51 GHz, respectively. In total, the excited modes are $TE_{\delta 11}$ at 7 GHz, $HE_{11\delta}$ at 9.85 GHz, and around 10 GHz, we have excited modes ($HEM_{01\delta}$, $EH_{11\delta}$, $TE_{1\delta 1}$, and $TE_{11\delta}$), as shown in Fig. 6. The TE_{102} and $TE_{\delta 21}$ modes are excited at 12.4 and 16 GHz [27], and finally the mode $TM_{01\delta}$ at 17.5 GHz (Fig. 6).

Figs. 7 and 8 illustrate respectively the measured and simulated gains in the broadside direction and efficiency of the presented antenna. The simulated gain assumes an ideal feeding network, whereas the measurements include the actual feeding network insertion loss, hence there are local discrepancies. The plot shows the calculated gain varying between 4.30 and 9.98 dBi with a maximum of 9.98 dBi at 15GHz, while the measured gain varies between 5.65 and 7.9 dBi in the band from 6 to17.5GHz, with a maximum of 7.9 dBi at 17.5 GHz. Additionally, the measured radiation efficiencies are over 75 % from 3.6 to18 GHz.

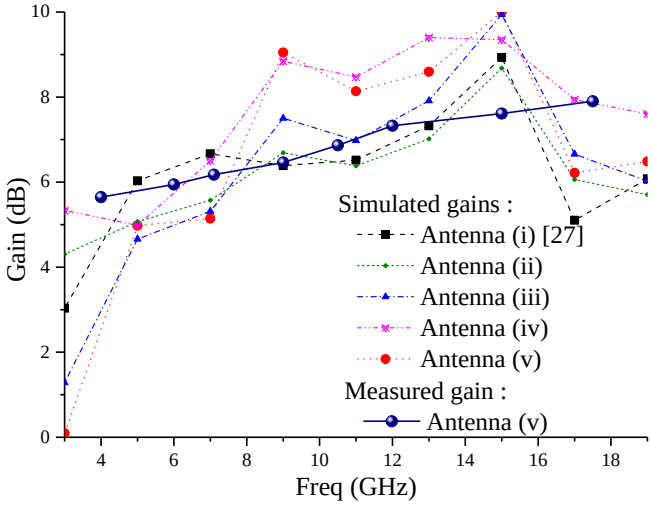

FIGURE 7. Measured and simulated gains of the proposed antennas.

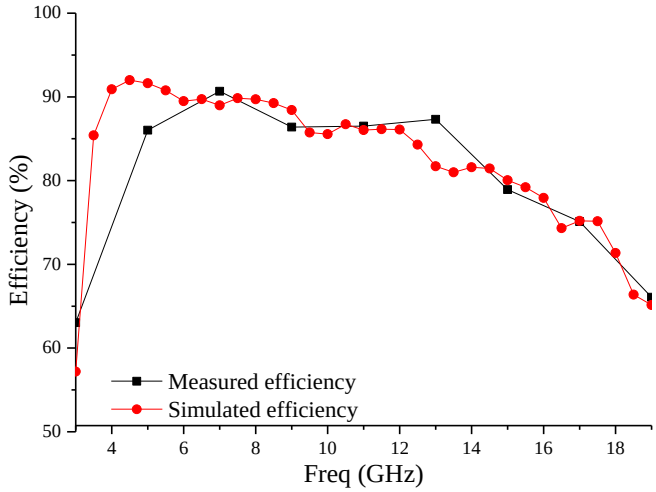

FIGURE 8. Measured and simulated efficiency of the proposed antenna.

This article has been accepted for publication in a future issue of this journal, but has not been fully edited. Content may change prior to final publication. Citation information: DOI 10.1109/ACCESS.2019.2949527, IEEE Access

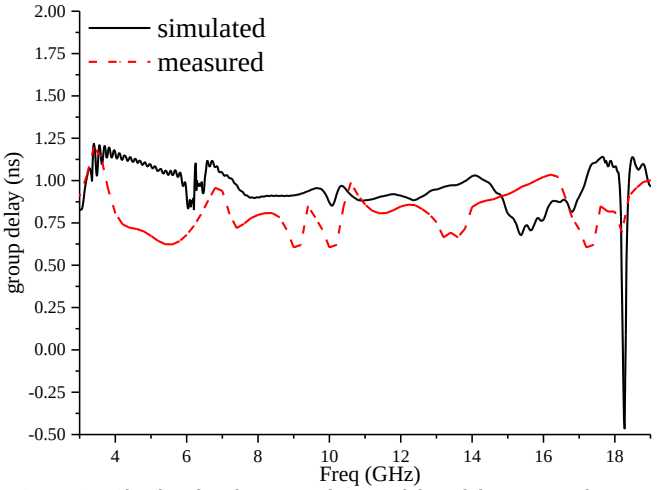

FIGURE 9. Simulated and measured group delay of the proposed antenna.

Form Fig. 9, the antenna provides linear S_{21} response and non-varying group delay response in the 3.6-18GHz, where maximum and minimum values of simulated group delay are 1.19 and 0.7 ns, respectively, whereas the measured are 1.19 and 0.66 ns, which shows an acceptable performance in time-domain.

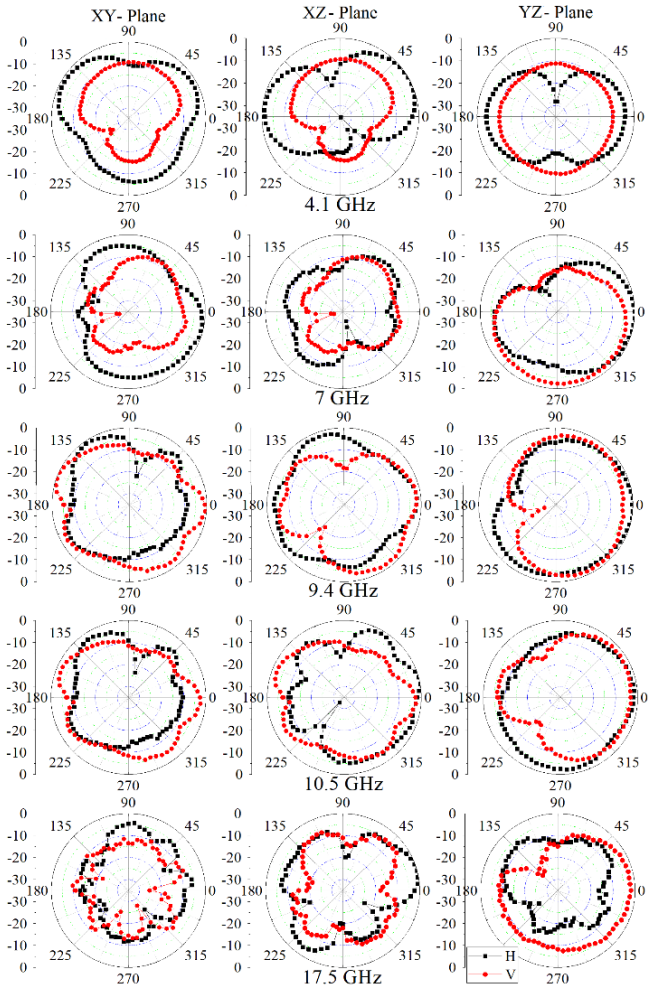

FIGURE 10. Measured radiation patterns of the proposed antenna. Left: xy-plane, middle: xz-plane and right: yz-plane.

Fig. 10 shows radiation patterns measured at frequencies 4.1, 7, 9.4, 10.5 and 17.5 GHz. This shows that the antenna has a wide radiation pattern with a maximum along the normal to the substrate, covering a half-space. In some cases, an almost omnidirectional radiation pattern is observed.

IV. EFFECT OF DRs NUMBER

The proposed arrangement of two slots feeding the two DRs gives an extra degree of freedom in the design procedure. The achieved higher bandwidth can be interpreted as the result of merging many resonating frequencies bands of the different parts constituting the antenna. Obviously, adding a second slot has resulted in increased bandwidth. Wherever each resonant frequency can be attributed to a relevant part of the antenna, the designer will have a wider scope to tailor the required extension of the bandwidth.

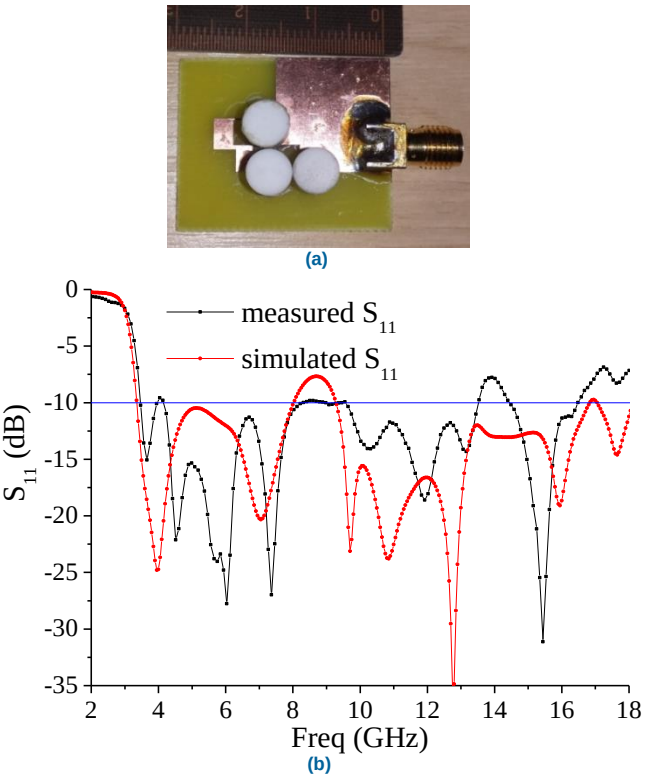

FIGURE 11. (a) Proposed antenna with three DRs (1st configuration). (b) Simulated and measured S_{11} of 3-DR antenna.

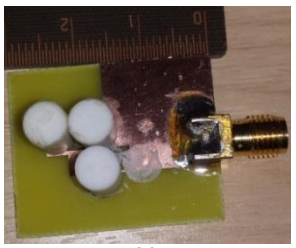

This article has been accepted for publication in a future issue of this journal, but has not been fully edited. Content may change prior to final publication. Citation information: DOI 10.1109/ACCESS.2019.2949527, IEEE Access

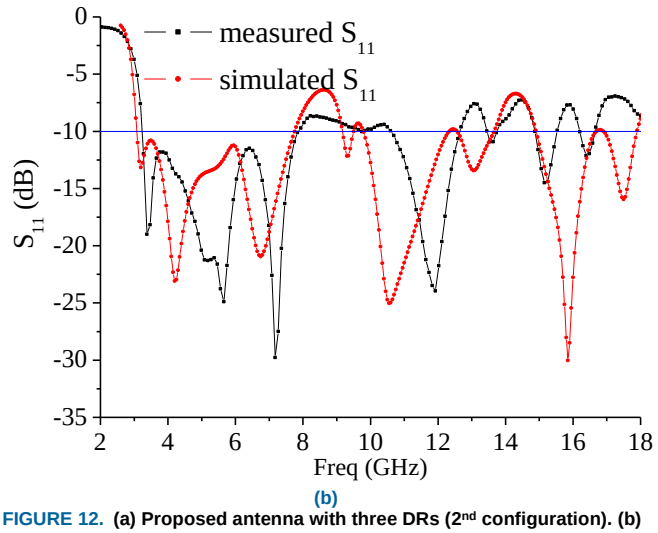

(b)

FIGURE 12. (a) Proposed antenna with three DRs (2nd configuration). (b) Simulated and measured S_{11} of 3-DR antenna.

While the resonating parts of the antenna: DRs, slots and feed line/stub are the most influential factors on the antenna characteristics, the effect of the DR number with a wide slot on S_{11} is also investigated.

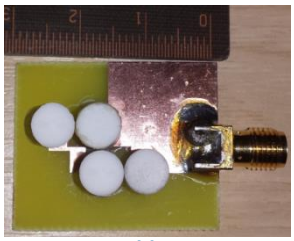

(a)

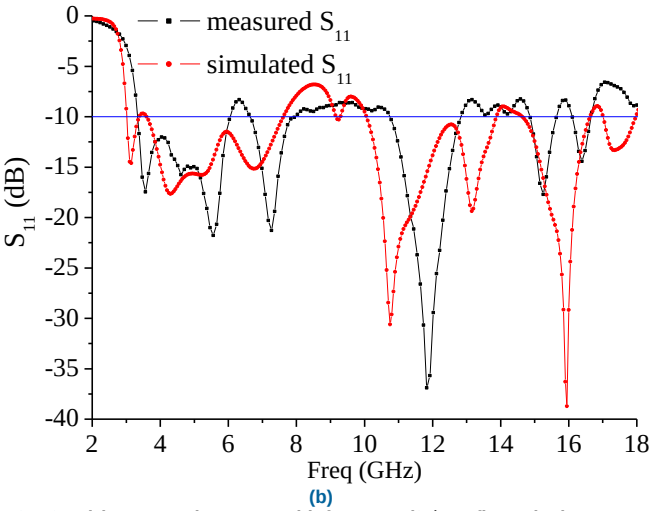

(b)

FIG. 12. **(a) Proposed antenna with four DRs (3rd configuration) (b)Simulated and measured S_{11} of 4-DR antenna.**

The DR number effect is very important compared to the slot, as is well illustrated by Figs. 11, 12 and 13.

For the first case (3-DR antenna configuration), we could theoretically have a bandwidth of 3.4-8.05 and 9.25-16.85GHz and experimentally 3.35-13.45 and 14.45-16.5GHz (Fig. 11). In the second configuration, the bandwidth is shifted to 3.05-7.85GHz and 9.15-12.3GHz; a slight variation between the theoretical and the experimental results is observed (Fig. 12).

For the third case (4-DR antenna configuration, Fig.13), the frequency is shifted down to 3GHz; but in this case the antenna bandwidth becomes relatively narrower.

The advantage of having a wide slot is to excite the lower frequencies and this can, with an adequate number of DRs, control the usable frequency band.

V. CONCLUSION

In this work, a compact dielectric resonator antenna for ultra-wideband applications has been studied. It has been shown that the use of dielectric resonators enhances the antenna performance. The asymmetric placement of the DR pair (three and four), the defected ground technique, the dimensions and the shape of the aperture together give designers more scope for the optimization process. More resonances can be generated and the bandwidth has thereby been improved. The obtained results show that an impedance bandwidth of 133.33%, covering the UWB 3.6 GHz to 18.0 GHz, and a maximum simulated and measured power gain of 9.9dBi and 7.9 dBi, respectively, have been achieved. The measured results of the prototype gave two bands extending from 3.55 to 13.05 GHz (114.46%) and from 14.3 to 16 GHz (11%).

ACKNOWLEDGMENT

This work has received funding from the European Union's Horizon 2020 research and innovation program under grant agreement H2020-MSCA-ITN-2016 SECRET-722424. This work is also funded by the FCT / MEC through national funds and when applicable co-financed by the ERDF, under the PT2020 Partnership Agreement under the UID / EEA / 50008/2019 project.

REFERENCES

[1] S. F. Jilani and A. Alomainy, "Millimetre-wave T-shaped MIMO antenna with defected ground structures for 5G cellular networks", IET Microwaves, Antennas & Propagation, vol. 12, no. 5, 2018, pp. 672-677.
[2] C. Zebiri, D. Sayad, N.T. Ali, M. Lashab, F. Benabdelaziz, R.A. Abd-Alhameed, I.T.E. Elfergani and J. Rodriguez, "Reduced ground plane aperture-coupled DRA fed by slotted microstrip for Ultra-Wideband application", 2017 11th European Conference on Antennas and Propagation (EUCAP), pp. 965-969, 2017.
[3] D. Guha, M. Biswas, and Y. M. M. Antar, "Microstrip patch antenna with defected ground structure for cross polarization suppression," IEEE Antennas and Wireless Propagat. Lett., vol. 4, pp. 455-458, 2005.
[4] D. Guha, S. Biswas, T. Joseph and M. T. Sebastian, "Defected ground structure to reduce mutual coupling between cylindrical dielectric resonator antennas," Electronic Lett., Vol. 44, No. 14, PP. 836-837, 2008.
[5] A. K. Gautam, A. Bisht, B. K. Kanaujia, "A wideband antenna with defected ground plane for WLAN/WiMAX applications," AEU-International Journal of Electronics and Communications, 2016, vol. 70, no 3, pp. 354-358.
[6] A Boutejdar and W Abd Ellatif, "A novel compact UWB monopole antenna with enhanced bandwidth using triangular defected microstrip structure and stepped cut technique", Microwave and Optical Technology Letters, 2016, vol. 58, no 6, pp. 1514-1519.

[7] W.-C. Liu, C.-M. Wu, Y. Dai, "Design of triple-frequency microstrip-fed monopole antenna using defected ground structure," IEEE Trans Antennas Propag, vol. 59, no. 7, (2011), pp. 2457-2463.

[8] W. Hu, Y.-Z. Yin, P. Fei, X. Yang, "Compact triband square-slot antenna with symmetrical L-strips for WLAN/WiMAX applications," IEEE antennas and wireless propagation letters, No. 11, 2010, pp. 462-465.

[9] M. K. Khandelwal, B. K. Kanaujia, and S. Kumar," Defected Ground Structure: Fundamentals, Analysis, and Applications in Modern Wireless Trends", International Journal of Antennas and Propagation Volume 2017, Article ID 2018527, 22 pages.

[10] N. P. Yadav, "Triple U-slot loaded defected ground plane antenna for multiband operations", Microwave and Optical Technology Letters, 2016, Vol. 58, No 1, PP. 124-128.

[11] V. Tiwari, K. Vyas, and N. Goyal. "Gain enhancement of a CPW-Fed horse shoe shaped slot antenna with defected ground structures for WiMax/WLAN applications", Recent Advances and Innovations in Engineering (ICRAIE), 2014. IEEE, 2014. pp. 1-5.

[12] A. Singh, and S. Singh, "A novel CPW-fed wideband printed monopole antenna with DGS", AEU-International Journal of Electronics and Communications, Vol. 69, No.1, 2015, PP.299-306.

[13] C. Zhang, J. Zhang, and L. Li, "Triple band-notched UWB antenna based on SIR-DGS and fork-shaped stubs", Electronics Letters, vol. 50, No. 2, pp. 67-69, 2014.

[14] D. H. Bi, Z. Y. Yu, S. G. Mo, X. C. Yin, "Two new ultra-wideband antennas with 3.4/5.5 GHz dual band-notched characteristics," Microwave Opt. Tech. Lett., Vol. 51, pp. 2942- 2945, 2009.

[15] A. Nouri, G. R. Dadashzadeh, "A compact UWB band-notched printed monopole antenna with defected ground structure",.IEEE antennas and wireless propagation letters, No. 10, 2011, pp.1178-1181.

[16] K. H. Chiang and K. W. Tam, "Microstrip monopole antenna with enhanced bandwidth using defected ground structure", IEEE antennas and wireless propagation letters, 2008, Vol. 7, pp. 532-535.

[17] C. Zebiri, M. Lashab, D. Sayad, I.T. E. Elfergani, A. Ali, M. Al Khambashi, J. Rodregiez, F. Benabdelaziz, R.A. Abd-Alhameed, "Bandwidth Enhancement of rectangular dielectric resonator antenna using circular and sector slot coupled technique," 12th European Conference on Antennas and Propagation (EuCAP 2018), IET, 2018, pp.1-4.

[18] C. Ozzaim, F. Ustuner, and N. Tarim, "Stacked conical ring dielectric resonator antenna excited by a monopole for improved ultrawide bandwidth". IEEE Transactions on Antennas and Propagation, 2013, vol. 61, no 3, p. 1435-1438.

[19] R. D. Gupta, M. S. Parihar, "Investigation of an asymmetrical E-shaped dielectric resonator antenna with wideband characteristics", IET Microwaves, Antennas & Propagation, 2016, vol. 10, no 12, p. 1292-1297.

[20] L. Lu, Y. C. Jiao, H. Zhang, R. Wang, and T. Li, "Wideband Circularly Polarized Antenna with Stair-Shaped Dielectric Resonator and Open-Ended Slot Ground", IEEE Antennas and Wireless Propagation Letters, 2016, vol. 15, p. 1755-1758.

[21] P. Suwanta, P. Krachodno, and R. Wongson, "Wideband Inverted L-shaped Dielectric Resonator Antenna for Medical Applications", In IEEE International Conference on Computational Electromagnetics (ICCEM). IEEE 2017, p. 188-189.

[22] R. Chakraborty, M. Pal, R. Ghatak, "An X-band dielectric resonator antenna using a single elliptical shaped dielectric resonator", AEU-International Journal of Electronics and Communications, 2018, vol. 83, p. 348-352.

[23] Y. Gao, Z. Feng, L. Zhang, "Compact asymmetrical T-shaped dielectric resonator antenna for broadband applications", IEEE Transactions on Antennas and Propagation, Vol. 60, No. 3, 2012, pp.1611-1615.

[24] A. A. Kishk, "Wideband dielectric resonator antenna in a truncated tetrahedron form excited by a coaxial probe", IEEE Trans. Antennas Propag., Vol. 51, No. 10, PP. 2907-2912, 2003.

[25] K. Trivedi, D. A. Pujara, "Design and Development of a Wideband Fractal Tetrahedron Dielectric Resonator Antenna with Triangular Slots", Progress In Electromagnetics Research, 2017, vol. 60, p. 47-55.

[26] A. H. Majeed, A. S. Abdallah, F. Elmegri, K. H. Sayidmarie, R. A. Abd-Alhameed, and J. M. Noras, "Aperture-Coupled Asymmetric Dielectric Resonator Antenna for Wideband Applications", IEEE Antennas and Wireless Propagation Letters, Vol. 13, May 2014, PP. 927-930.

[27] C-E Zebiri, M. Lashab, D. Sayad, I.T.E. Elfergani, K. H. Sayidmarie, F. Benabdelaziz, R. A. Abd-Alhameed, J. Rodriguez, J. M. Noras "Offset Aperture-Coupled Double-Cylinder Dielectric Resonator Antenna with Extended-Wideband", IEEE Transactions on Antennas and Propagation, 2017, Vol. 65, No 10, PP. 5617-5622.

[28] N. Yang, K. W Leung, N. Wu, "Pattern-Diversity Cylindrical Dielectric Resonator Antenna Using Fundamental Modes of Different Mode Families," IEEE Transactions on Antennas and Propagation, 2019

[29] D. Guha, B. Gupta and Y. M. M. Antar, "Hybrid monopole-DRAs using hemispherical/conical-shaped dielectric ring resonators: Improved ultrawideband designs", IEEE Transactions on Antennas and Propagation, Vol. 60, No. 1, PP. 393-398, 2012.

[30] C. Zebiri, F. Benabelaziz, M. lashab, D. Sayad, F. Elmegri, I. T. E. Elfergani, N. T. Ali, A. S. Hussaini, R. A. Abd-Alhameed and J. Rodriguez, "Aperture-Coupled Asymmetric Dielectric Resonator Antenna with Slotted Microstrip line for Enhanced Ultra Wideband", In Antennas and Propagation (EuCAP), 2016 10th European Conference on, IEEE, PP. 1-3, April 2016.

[31] I. Elfergani, A. S. Hussaini, J. Rodriguez, R. Abd-Alhameed, (eds.): Antenna Fundamentals for Legacy Mobile Applications and Beyond, 1st Ed. Springer, Cham (2018). https://doi.org/10.1007/978-3-319-63967-3.

[32] G. Almpanis, C. Fumeaux, and R. Vahldieck, "Offset cross-slot-coupled dielectric resonator antenna for circular polarization", IEEE Microwave and Wireless Components Letters, Vol. 16, No. 8, PP. 461-463, 2006.

[33] K. M. Luk and K.W. Leung, "*Dielectric Resonator Antennas",* Hertfordshire, U.K.: Research Studies Press Ltd., 2002.

[34] G. P. Junker, A. A. Kishk, A. W. Glisson, D. Kajfez, "Effect of an air gap around the coaxial probe exciting a cylindrical dielectric resonator antenna", IEE Electronics Letters, Vol. 30, No. 3, Feb. 1994, pp. 177-178.

[35] K. K. Chow, "On the solution and field patterns of cylindrical dielectric resonators," IEEE Trans. Microw. Theory Tech., vol. 14, no. 9, pp. 439, Sep. 1966.

[36] Y. Chen and C. F Wang. (2015). "Characteristic modes: Theory and applications in antenna engineering". John Wiley & Sons.

[37] A. A. Kishk, M. R. Zunoubi and D. Kajfez, "A numerical study of a dielectric disk antenna above a grounded dielectric substrate," IEEE Trans. Antennas Propagat., Vol. AP-41, 813-821, June 1993.

[38] M. Chauhan, A. K. Pandey, B. Mukherjee, "A novel Compact Cylindrical Dielectric Resonator Antenna for Wireless Sensor Network application", IEEE sensors letters, 2018, vol. 2, no 2, p. 1-4.

[39] A. Iqbal, A. Smida, O. A. Saraereh, Q. H. Alsafasfeh, N. K. Mallat, and B. M. Lee, "Cylindrical Dielectric Resonator Antenna-Based Sensors for Liquid Chemical Detection", Sensors, 2019, vol. 19, no 5, p. 1200.

[40] B. J. Liu, J. H. Qiu, C. H. Wang, W. Li, G. Q. Li, "Polarization-Reconfigurable Cylindrical Dielectric Resonator Antenna Excited by Dual Probe with Tunable Feed Network", IEEE Access, 2019, vol. 7, pp. 60111-60119.

[41] G. P. Junker, A. A. Kishk and A. W. Glisson, "Input impedance of aperture coupled dielectric resonator antenna," IEEE Trans. on Antennas and Propagation, Vol. AP-44, No. 5, 600-607, May 1996.

[42] A. A. Kishk, Glisson, A. W. and Junker, G. P. "Bandwidth enhancement for split cylindrical dielectric resonator antennas", Progress In Electromagnetics Research, 2001, vol. 33, pp. 97-118.

[43] R. K. Mongia and P. Bhartia, "Dielectric resonator antennas - a review and general design relations for resonant frequency and bandwidth," Int. J. Microw. Millimeter-Wave Comput. Aided Eng., vol. 4, no. 3, pp. 230-247, Jul. 1994.

[44] Y. Wang, S. Liu, T. A. Denidni, Q. Zeng, and G. Wei, "Integrated Ultra-Wideband Planar Monopole with Cylindrical Dielectric Resonator Antennas." Progress in Electromagnetics Research C, vol. 44, 2013, PP. 41-53.

[45] R. K. Mongia, "Theoretical and experimental resonant frequencies of rectangular dielectric resonators," IEE Proc. H Microwav. Antennas Propag., Vol. 139, No. 1, pp. 98-104, Feb. 1992.

[46] R. K. Mongia, A. Ittipiboon, and M. Cuhaci, "Measurement of radiation efficiency of dielectric resonator antennas," IEEE Microwave and Guided Wave Letters, Vol. 4, No. 3, 80-82, 1994.

[47] J. Van Bladel, "On the Resonances of a Dielectric Resonator of Very High Permittivity," Microwave Theory and Techniques, IEEE Transac. on Microwave, Theory and Techniques, Vol.23, No.2, PP. 199- 208, 1975.

[48] A. A. Kishk, B. Ahn and D. Kajfez, “Broadband stacked dielectric resonator antennas,” Electron. Lett., Vol. 25, PP. 1232-1233, Aug. 1989.
[49] S. M. Shum and K. M. Luk, “Stacked annular-ring dielectric resonator antenna excited by axi-symmetric coaxial probe,” IEEE Trans. Antennas Propag., Vol. 43, No. 8, PP. 889-892, 1995.
[50] K. W. Leung, K. M. Luk, K. Y. Chow and E. K. N. Yung, “Bandwidth enhancement of dielectric resonator antenna by loading a low-profile dielectric disk of very high permittivity,” Electron. Lett., Vol. 33, PP. 725-726, Apr. 1997.
[51] A. Sangiovanni, J. Y. Dauvignac and C. Pichot, “Stacked dielectric resonator antenna for multifrequency operation,” Microw. Opt. Technol. Lett., Vol. 18, PP. 303-306, Jul. 1998.
[52] A. A. Kishk, X. Zhang, A.W. Glisson and D. Kajfez, “Numerical analysis of stacked dielectric resonator antennas excited by a coaxial probe for wide-band applications,” IEEE Trans. Antennas Propag., Vol. 51, No. 8, PP. 1996-2006, Aug. 2003.
[53] A. A. Kishk, A. W. Glisson and G.P. Junker, "Study of broadband dielectric resonator antennas", 1999 Antenna applications symposium, Sept. 1999, Allerton Park, Monticello (Il), PP. 45-68.
[54] R. K. Mongia and A. Ittipiboon, "Theoretical and experimental investigations on rectangular dielectric resonator antennas", IEEE Transactions on antennas and propagation, Vol. 45, No. 9, Sept. 1997, PP. 1348-1356.